Design of UAV Flight State Recognition System for Multi-sensor Data Fusion

Zhuoyong Shi, Guoqing Shi, Jiandong Zhang, Dinghan Wang, Tianyue Xu, Longmeng Ji, and Yong Wu

***Abstract*—With the impact of artificial intelligence on the traditional UAV industry, autonomous UAV flight has become a popular research field at present. Based on the demand for research on key technologies for autonomous UAV flight, this paper studies UAV flight state recognition. This paper is based on multi-sensor acquisition of UAV on-board information, and uses the collected information for data fusion to complete UAV flight state identification. Firstly, UAV flight data acquisition and data preprocessing are carried out; secondly, UAV flight trajectory features are extracted based on multidimensional data fusion; finally, UAV flight state recognition model based on PCA-DAGSVM model is established. The results show that the algorithm based on multi-sensor data fusion has good recognition effect in the UAV flight state recognition problem. The recognition accuracy of the algorithm exceeds that of the random forest model, and its accuracy in the training set of UAV flight state recognition is more than 90%, and its accuracy in the test set is more than 80%.**

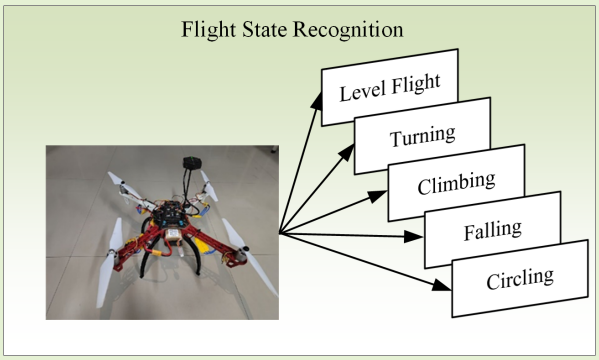

***Index Terms*—UAV; Pattern Recognition; Multi-Sensor; PCA-DAGSVM Model; Data Fusion**

I. Introduction

UAV (unmanned aerial vehicle) is an aerial vehicle that does not require a pilot to be aboard [1, 2] and can be remotely controlled or autonomously pre-programmed to perform a variety of tasks. The development of UAVs has benefited from advances in a number of fields such as aviation technology, computer science, electronics and sensor technology. UAVs were initially used in the military as a tool for intelligence reconnaissance, targeting and aerial attack [3]. However, with the advancement of technology and the reduction of costs, drones are gradually being widely used in the civilian sector [4, 5]. Nowadays, UAVs play an important role in aerial photography, cargo transportation, agriculture, scientific research, disaster monitoring and rescue, and film and television filming [6, 7]. A safety monitoring system is a system that is used to supervise the parameters of the machine movement process, which allows the monitoring and control of the relevant parameters during the operation of the machine [8-13].

Flight state recognition of UAVs belongs to the field of pattern recognition, which was first widely used in the aerospace field to monitor the flight state of air and space electronic devices [14]. Related scholars in the field of pattern recognition use algorithms such as support vector machines [15], decision trees [16], random forests [17], and artificial neural networks [18] to conduct research.

In pattern recognition, Shi [19] applied wearable devices in pattern recognition for table tennis players' motor skills, using an enhanced support vector machine model, showing its feasibility in skill classification. Rovinska [20] utilized physiological signals from wearables to judge human emotions, employing a self-encoder model that notably improved recognition accuracy. Vellenga [21] developed a predictive model for drivers' braking intentions during vehicle operation, addressing the need for reliable intention recognition.

The above literature is a review of the current state of research by current scholars in the areas of pattern recognition and UAV trajectory prediction. Based on the need for research in areas related to autonomous flying UAVs, this paper investigates two key areas of autonomous flying UAVs, flight state recognition and UAV trajectory prediction.

The main contributions and innovations are listed below:

1) Designed the UAV record data acquisition system, which can complete the accurate monitoring of UAV data.

2) The extraction of UAV trajectory features is completed by using data fusion.

3) Improved the support vector machine model based on directed acyclic graph, and completed the identification of UAV flight state.

The rest of this article is organized as follows. The second part is the acquisition and pre-processing of UAV data, which introduces the data acquisition system built in this study and the content of outlier rejection, missing term interpolation and high

This work was supported by the Natural Science Basic Research Program of Shaanxi (Program No. 2022JQ-593) and the Aeronautical Science Foundation of China (Program No. 20220013053005) (Corresponding author: Jiandong Zhang)

Zhuoyong Shi is studying for an MPhil degree in electronic science and technology at Northwestern Polytechnical University, China (e-mail: shizy@mail.nwpu.edu.cn).

Guoqing Shi is an associate professor at the School of Electronic Information, Northwestern Polytechnical University, China. (e-mail: shiguoqing@nwpu.edu.cn)

Jiandong Zhang is an associate professor at the School of Electronic Information, Northwestern Polytechnical University, China. (e-mail: jdzhang@nwpu.edu.cn)

frequency noise filtering of the acquired data. The third part is the UAV flight state recognition model, which constructs the UAV feature information based on feature engineering and predicts the UAV flight state based on the improved support vector machine model with directed acyclic graph. The fourth part presents the results of the experiment and analyses the results of the experiment. Finally, Section 5 concludes the paper.

II. Data Acquisition and Preprocessing

A. UAV data acquisition

Build UAV data acquisition system mainly includes position module air pressure module and attitude module, its structure is shown in Figure 1.

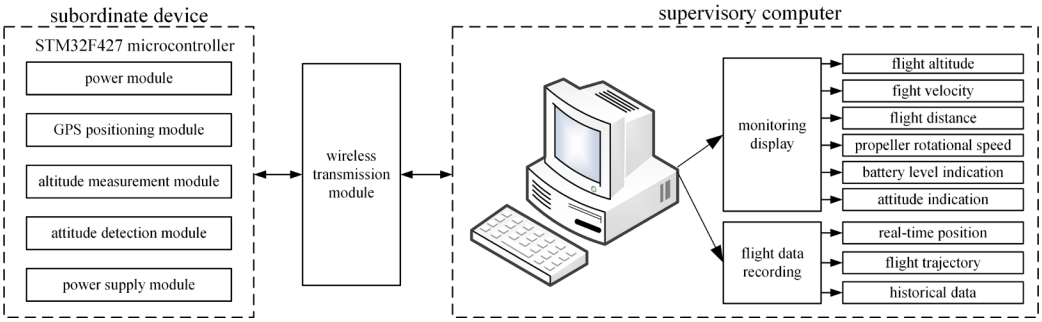

Fig. 1. UAV data acquisition system

As shown in Figure 1, it can be seen that the subordinate device contains power module, GPS positioning module, altitude measurement module, attitude detection model and power supply module; the monitoring of the data is completed through the wireless transmission system; and the upper device displays and saves the collected data.

The UAV monitoring system is built based on this system block diagram as shown in Fig. 2.

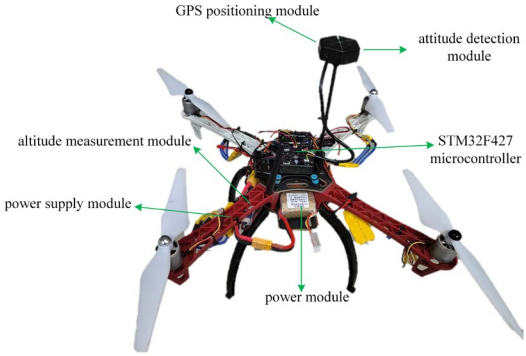

Fig. 2. The UAV monitoring system

As shown in Figure 2, the UAV monitoring system contains a power module, a GPS position module, an altitude measurement module, an attitude detection model, and a power supply module.

The list of collected data is used for the study of this paper and the list of data is shown in Table 1.

TABLE I
ACQUISITION DATA OF UAV

Data name	Data Volume	Time Resolution
GPS data	10000	0.1s
Barometer Data	10000	0.1s
Acceleration Data	10000	0.1s
Barometric Data	10000	0.1s

As shown in Table 1, the UAV GPS information, Barometer information, Acceleration information, Barometric information, the amount of data collected is 10000, and the time resolution of the collection is 0.1s.

B. Collection data pre-processing

Due to factors such as sensor acquisition error or data remote transmission process, the collected UAV trajectory data may generate noise, so it is necessary to carry out data preprocessing after collecting UAV data. Data preprocessing mainly includes three parts: eliminating abnormal data, repairing missing data and filtering high frequency noise, and finally outputting the repaired data after the preprocessing is completed.

1) Abnormal data rejection

For a set of data n samples $\{x_1, x_2, \ldots, x_n\}$ returned by the UAV, after returning the data, anomalous data needs to be culled from the retainer. According to the 3σ criterion, the data in the $(EX-3\sigma, EX+3\sigma)$ interval in X_i is retained, the data outside the interval is considered to be abnormal data and eliminated, and the X_i abnormal data outside the interval and the corresponding x_{i+1} data are eliminated, so as to realize the elimination of abnormal data.

2) Missing data repair

After the outliers are removed, the data at the removed locations need to be repaired by interpolating the missing data using the Newton interpolation method, and finally the repaired data are output.

Based on Newton's interpolation method, a third-order difference quotient table is constructed to repair the function values of the missing data, so as to achieve data interpolation estimation of the missing data locations.

3) High frequency noise filtering

Based on that, an adaptive smoothing filtering method is used to update the filtering parameters by increasing the threshold value in order to adapt to the real-time signal. The new output value is defined as the current sample value and the previous output value weighted to obtain the current output value. The filtered output is shown in the formula.

$$Y(n) = m \bullet X(n) + (1-m) \bullet Y(n-1) \quad (1)$$

In formula (1), Y(n) is the filter output value, m is the filter coefficient between the interval [0,1], X(n) is the current sample value, and Y(n-1) is the previous filter output value.

III. UAV Flight States Recognition Model

A. Data fusion-based UAV trajectory feature extraction

Data fusion refers to the overall assessment that results from the detection and correlation of data information from multiple sources and levels and comprehensive analysis. In the field of UAV aerial data, UAV data are collected by sensors as position information, angular velocity information, acceleration information, and air pressure information, and the motion parameters during UAV flight are fused and solved by data layer fusion so as to extract UAV trajectory characteristics. The UAV flight data fusion hierarchy is shown in Figure 3.

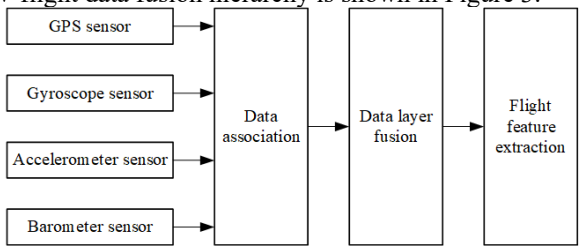

Fig. 3. UAV flight data fusion hierarchy

The motion parameters during UAV flight mainly include position in space, velocity, Euler angle, acceleration, acceleration direction, short-term curvature, etc.

The fusion of UAV flight data can achieve feature extraction of sensor data, and the extracted UAV flight data features include position, velocity, Euler angle, acceleration, direction of travel, and curvature in space.

1) Extraction of UAV spatial location

For the GPS latitude and longitude information collected by the data acquisition system, the plane coordinates of the UAV can be calculated by using the conversion of latitude and longitude and plane coordinate system. For the collected air pressure information, the relationship between air pressure and altitude can be obtained by using the atmospheric pressure-altitude formula, and the atmospheric pressure-altitude formula is shown in formula (2).

$$P = P_0 \times \left(1 - \frac{L * h}{T_0}\right)^{\frac{g*M}{R*L}} \tag{2}$$

In formula (2), the P_0 is the standard atmospheric pressure at sea level; the h is the altitude; the L is the temperature decreasing rate, about 0.0065 K/m in dry air; the T_0 is the standard temperature at sea level; the g is the acceleration of gravity at the Earth's surface, about $9.8 m/s^2$; the M is the molar mass, about 0.0289644 kg/mol; and the R is the universal gas constant, about 8.31447 .

The height solution formula is shown in formula (3).

$$z = 4.43 \times 10^4 \times (1 - 9.87 \times 10^{-6} P)^{\frac{1}{5.256}} \tag{3}$$

2) Extraction of UAV speed

The navigation speed of the UAV in space is defined as the derivative function of the displacement in each direction with respect to time. Considering that the UAV data acquisition system collects navigation data as discrete data, the ratio of the second-order backward difference of the displacement in each direction and the sampling interval is used as the speed in each direction, and the space navigation speed of the UAV is shown in formula (4).

$$\begin{cases} v_x(k) = \dfrac{\nabla x(k)}{T} \\ v_y(k) = \dfrac{\nabla y(k)}{T} \\ v_z(k) = \dfrac{\nabla z(k)}{T} \end{cases} \tag{4}$$

In formula(4), $\nabla f(k)$ denotes the second-order backward differencing, in other words, that is $\nabla f(k) = f(k) - f(k-1)$, T is the sampling interval.

3) UAV spatial attitude angle extraction

The attitude angle of the UAV in the air is calculated by the collected angular velocity information in UAV space, and the UAV attitude angle is solved as shown in equation (5).

$$\begin{cases} \theta_x(t) = \theta_x(0) + \int_0^t \omega_x(\tau) d\tau \\ \theta_y(t) = \theta_y(0) + \int_0^t \omega_y(\tau) d\tau \\ \theta_z(t) = \theta_z(0) + \int_0^t \omega_z(\tau) d\tau \end{cases} \tag{5}$$

Considering that the UAV data acquisition system collects angular velocity data as discrete data, the integration of angular velocity in each direction over a period of time is approximated as the sum of the sampled values of each angular velocity in that time period. Based on this, the sum of the accumulated angular velocity in each direction over time and the initial attitude is used as the attitude angle in each direction, and the UAV spatial attitude angle is shown in formula (6).

$$\begin{cases} \theta_x(n) = \theta_x(0) + \sum_{i=1}^{n} \omega_x(i) \\ \theta_y(n) = \theta_y(0) + \sum_{i=1}^{n} \omega_y(i) \\ \theta_z(n) = \theta_y(0) + \sum_{i=1}^{n} \omega_y(i) \end{cases} \tag{6}$$

4) UAV navigation acceleration extraction

The navigation acceleration of the UAV in space is defined as the derivative function of velocity in each direction with respect to time, and also the second-order derivative function of displacement in each direction with respect to time. Considering that the UAV data acquisition system collects navigation data as discrete data, the ratio of the second-order backward difference of displacement in each direction to the sampling interval is used as the acceleration in each direction, and the space navigation acceleration of the UAV is shown in formula (7).

$$\begin{cases} a_x(k) = \dfrac{\nabla v_x(k)}{T} = \dfrac{\nabla_2 x(k)}{T} \\ a_y(k) = \dfrac{\nabla v_y(k)}{T} = \dfrac{\nabla_2 y(k)}{T} \\ a_z(k) = \dfrac{\nabla v_z(k)}{T} = \dfrac{\nabla_2 z(k)}{T} \end{cases} \tag{7}$$

In formula (7), $\nabla_2 f(k)$ denotes the second-order backward difference, that is $\nabla_2 f(k) = \nabla f(k) - \nabla f(k-1)$.

5) UAV flight trajectory curvature extraction

The UAV trajectory curvature is used to measure the short-term time velocity excursion of the UAV, and the UAV

trajectory curvature can be approximated by the schematic diagram shown in Figure 4.

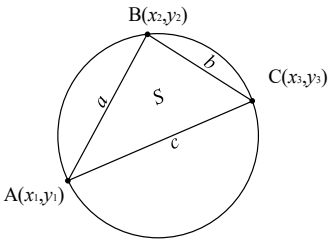

Fig. 4. Schematic diagram of flight curvature calculation

The radius of curvature is solved according to the data of the three points forming the external circle of the triangle as shown in Figure 4, and the radius of curvature is shown in formula(8).

$$R = \frac{abc}{4S} \tag{8}$$

The formula for calculating the area of a triangle from three points is shown in formula (9).

$$S = \left| \frac{x_1y_2 + x_2y_1 + x_3y_1 - (y_1x_2 + y_2x_3 + y_3x_1)}{2} \right| \tag{9}$$

The curvature of the drone flight trajectory can be approximated as shown in formula (10).

$$k = \frac{2(x_1y_2 + x_2y_1 + x_3y_1 - (y_1x_2 + y_2x_3 + y_3x_1))}{abc} \tag{10}$$

The spatial position of the UAV is obtained by converting the barometric data to the z-axis position, and the spatial position of the UAV can be obtained by combining the plane position; the spatial velocity of the UAV is obtained by the first-order difference of the UAV position; the attitude angle of the UAV is calculated by the cumulative sum of the initial attitude and the angular velocity. The spatial acceleration of the UAV is obtained by the first-order difference of the velocity. The curvature of the drone is solved by the relationship between three consecutive sampling points. The definitions of position, velocity, Euler angle, acceleration, and curvature in UAV space and the calculation formulas are shown in Table 2.

TABLE II
DATA CHARACTERISTICS OF THE UAV DURING FLIGHT

Data name	Definition	Calculation formula	
Altitude	Position of UAV in space	$z = 4.43\times10^4 \times (1-9.87\times10^{-6}P)^{\frac{1}{5.256}}$	(11)
Speed	Change rate of UAV position with time	$\begin{cases} v_x(k) = \frac{\nabla x(k)}{T} \\ v_y(k) = \frac{\nabla y(k)}{T} \\ v_z(k) = \frac{\nabla z(k)}{T} \end{cases}$	(12)
Posture angle	The angle of the UAV body coordinate system relative to the geodetic coordinate system	$\begin{cases} \theta_x(n) = \theta_x(0) + \sum_{i=1}^{n} \omega_x(i) \\ \theta_y(n) = \theta_y(0) + \sum_{i=1}^{n} \omega_y(i) \\ \theta_z(n) = \theta_y(0) + \sum_{i=1}^{n} \omega_y(i) \end{cases}$	(13)
Acceleration	Change rate of UAV speed with time	$\begin{cases} a_x(k) = \frac{\nabla v_x(k)}{T} = \frac{\nabla_2 x(k)}{T} \\ a_y(k) = \frac{\nabla v_y(k)}{T} = \frac{\nabla_2 y(k)}{T} \\ a_z(k) = \frac{\nabla v_z(k)}{T} = \frac{\nabla_2 z(k)}{T} \end{cases}$	(14)
Curvature	Curved degree of UAV motion curve	$k = \frac{2(x_1y_2 + x_2y_1 + x_3y_1 - (y_1x_2 + y_2x_3 + y_3x_1))}{abc}$	(15)

After filtering the UAV acquisition signal and extracting the data features to construct the UAV trajectory features, 75 feature quantities are extracted as the data features in Table 2. The mean, variance, maximum, minimum, peak and valley values of 13 data features such as position, velocity, Euler angle, acceleration and curvature in UAV space after adding the sliding window and the mean, variance, maximum, minimum, peak and valley values of synthetic velocity and synthetic acceleration are extracted respectively.

B. UAV trajectory feature downscaling

In the field of machine learning, overlearning directly affects classification accuracy and can increase the task size of machine learning. PCA (Principal Component Analysis) is a typical unsupervised dimensionality reduction algorithm that can reduce multiple metrics into several principal components, which are linearly combined from the original variables without any relationship between them and can reflect most of the useful information in the original data. The dimensionality of the UAV trajectory feature data extracted in this study is 75 dimensions, so this paper uses a principal component analysis model to reduce the dimensionality of the trajectory feature to construct an effective UAV trajectory feature.

Based on the metrics in the UAV flight data and the classification labels of the UAV flight states to form a matrix, each element of the matrix is subtracted from the mean value of that column of the matrix to obtain the decentered matrix as shown in formula (16).

$$X_{ij}=\begin{bmatrix} x_{11}-\frac{1}{m}\sum_{i=1}^{m}x_{i1} & x_{12}-\frac{1}{m}\sum_{i=1}^{m}x_{i2} & \cdots & x_{1n}-\frac{1}{m}\sum_{i=1}^{m}x_{in} \\ x_{21}-\frac{1}{m}\sum_{i=1}^{m}x_{i1} & x_{22}-\frac{1}{m}\sum_{i=1}^{m}x_{i2} & \cdots & x_{2n}-\frac{1}{m}\sum_{i=1}^{m}x_{in} \\ \vdots & \vdots & \ddots & \vdots \\ x_{m1}\frac{1}{m}\sum_{i=1}^{m}x_{i1} & x_{m2}-\frac{1}{m}\sum_{i=1}^{m}x_{i2} & \cdots & x_{mn}-\frac{1}{m}\sum_{i=1}^{m}x_{in} \end{bmatrix} \quad (16)$$

The covariance matrix is calculated from the decentered matrix of the UAV flight data as shown in formula (17)

$$C=\frac{1}{m-1}X^{T}X \quad (17)$$

The eigenvalue λ_k of the covariance matrix C and the corresponding eigenvector v_k are obtained by eigen decomposition of the covariance matrix C, which is shown in formula (18).

$$Cv_k=\lambda_k v_k \quad (18)$$

The contribution of the i-th component to the total component c_i is defined as shown in formula (19).

$$c_i=\frac{\lambda_i}{\sum_{k=1}^{p}\lambda_k}(i=1,2,\ldots,p) \quad (19)$$

In formula(19), $\lambda_i(i=1,2,\ldots,p)$ is the eigenvalue of the covariance matrix R.

The cumulative contribution margin is defined as shown in formula (20).

$$C_i=\frac{\sum_{k=1}^{i}\lambda_k}{\sum_{k=1}^{p}\lambda_k}(i=1,2,\ldots,p) \quad (20)$$

c_i is sorted in order from largest to smallest, and the cumulative contribution is cumulated sequentially, and when the cumulative contribution exceeds 85% of the cumulative contribution, it is used as the principal component of the motion feature constructed by the UAV.

Principal component analysis is used to construct UAV trajectory features to improve machine learning accuracy. The UAV trajectory features are analyzed and the information retention rate of the principal components is set to 85%, at which point the features are reduced to 14 dimensions.

C. UAV flight states classification

The flight states of UAVs mainly include five flight states, namely, level flight climbing turning circling and descending, and common machine learning identification and classification models include support vector machine model, random forest model, etc.

In the support vector machine, for a given binary data set $D=\{(x_i,y_i)\}_{i=1}^{N}$, where $y_i\epsilon\{+1,-1\}$, if the two samples are linearly separable, there is a hyperplane as shown in equation (21).

$$\omega^{T}x+b=0 \quad (21)$$

If the two types of samples are linearly separable, then there is $y_i(\omega^{T}x+b)>0$ for each sample, and the interval γ is defined as the distance from each sample in the data set to the segmentation hyperplane, and the interval γ is shown in formula (22).

$$\gamma_i=\frac{\left\|\omega^{T}x_i+b\right\|}{\|\omega\|}(i=1,2,\ldots,N) \quad (22)$$

Define the interval γ as the shortest distance from all samples in the entire dataset to the segmented hyperplane, as shown in equation (23).

$$\gamma=\min\gamma_i(i=1,2,\ldots,N) \quad (23)$$

Data classification is achieved by finding a most suitable hyperplane. This hyperplane should satisfy the maximum interval γ, and the division of the two data sets divided by the hyperplane is the most stable and robust, that is, the optimization equation (24) is solved.

$$\begin{cases}\max\gamma \\ s.t.\gamma_i\geq\gamma\end{cases} \quad (24)$$

The hyperplane parameter ω of $\gamma_i=\frac{\left\|\omega^{T}x_i+b\right\|}{\|\omega\|}(i=1,2,\ldots,N)$ makes $\|\omega\|\times\gamma=1$ hold, and the optimization equation can be simplified as shown in equation (25).

$$\begin{cases}\max\frac{1}{\|\omega\|^{2}} \\ s.t.y_i(\omega^{T}x+b)\geq 1\end{cases} \quad (25)$$

For a linearly separable data set, there are many segmentation hyperplanes, but the hyperplane with the largest interval is unique, which ensures the uniqueness of the support vector machine model for data set partitioning.

Support vector machine model is used to classify for the five flight states of UAVs, but the motion pattern of UAVs is not a binary case, so the traditional support vector machine model needs to be improved. The core of the direct method is to modify the objective function to integrate the multi-classification problem into one function, but the computational complexity is high and the confusion phenomenon is easy to occur. Considering that there are only five flight states of UAVs, the indirect method is chosen to implement the multi-classification problem of UAV flight states by support vector machines. In the indirect method, the improved DAGSVM model based on directed acyclic graphs outperforms the one-to-one and one-to-many indirect classifiers in solving the score-based, omission-based classification problems. The above analysis introduces a directed acyclic graph structure to solve the drawback that the support vector machine model can only perform binary classification. This paper classifies five flight states during UAV flight based on the DAGSVM (Directed Acyclic Graph Support Vector Machine) model. The five UAV flight states of climb, level flight, turn, circling and descent are recorded as A, B, C, D and E, respectively, and their

corresponding directed acyclic diagrams are classified as shown in Figure 5.

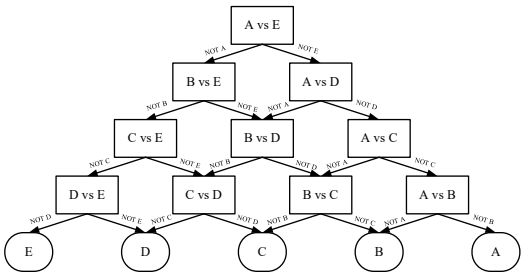

Fig. 5. Directed acyclic graph classification topology

As shown in Figure 5, the DAGSVM model-based directed acyclic graph structure is used to classify and identify the five flight states of the UAV 10 times to complete the identification of the UAV state.

IV. Experimental Results and Analysis

Machine learning is performed by DAGSVM model to achieve the classification recognition of UAV flight states. The five motion modes of UAV include climb, level flight, circling, turn and descent. The input data are 5000 sets of 14-dimensional samples of UAV navigation data with known flight states labels during UAV navigation, including 1000 sets of each of the five flight states data, and the data are divided into training and test sets according to the ratio of 80% and 20%. The loss function uses a 0-1 loss function, and the loss function between the true distribution y and the predicted distribution $f(x;\theta)$ of the labels is shown in equation (26).

$$L(y, f(x;\theta)) = \begin{cases} 0 & if\, y = f(x;\theta) \\ 1 & if\, y \neq f(x;\theta) \end{cases} \tag{26}$$

The number of classifier errors is shown in formula (27).

$$n = \sum_{i=1}^{m} \mathcal{L}(y_i, f_i(x;\theta)) \tag{27}$$

In formula (27), m is the number of samples.

According to the Directed Acyclic Graph Support Vector Machine model in 3.3, the five flight states of climb, level flight, circling, turn and descent of the UAV are classified and identified. The confusion matrix heat map of the training and test sets of the classifier classification results is shown in Figure 6.

a) Heat map display of confusion matrix for training set

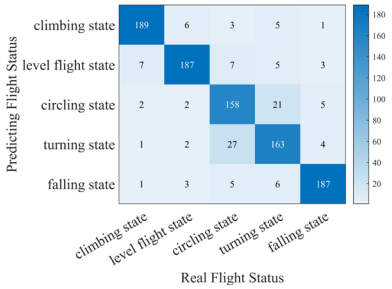

b) Heat map display of confusion matrix for testing set

Fig. 6. UAV flight states classification results

As shown in Figure 6, the number of climb training accuracy is 794 and the number of test accuracy is 189; the number of level flight training accuracy is 789 and the number of test accuracy is 187; the number of circling training accuracy is 746 and the number of test accuracy is 158; the number of turn training accuracy is 757 and the number of test accuracy is 163; and the number of descent training accuracy is 791 and the number of test accuracy is 187.

In the classification model, there are some metrics to measure the classification effectiveness of the classification model, such as precision, recall, F1 metric, etc.

The F1 metric for any classification in this classifier is defined as the ratio of the true category of that classification to the linear combination of the predicted and true categories of that classification, and the F1 metric is shown in formula (28).

$$P = \frac{2TP}{2TP + 2\alpha FN + 2(1-\alpha)FP} \times 100\% \tag{28}$$

In formula (28), TP is the number of true categories in the type, FP is the number of predicted categories in the category but the true categories are not in the category, FN is the number of true categories in the category but the predicted categories are not in the category, and α is a weighting factor for precision and recall, taking values between 0,1, used to determine the preference for precision and recall in the final classifier's metric.

In UAV flight state recognition, it is more sensitive to the accuracy of true classification recognition, i.e., the weight for the accuracy rate should be greater than the recall rate, so set the weight coefficient $\alpha = 0.7$ for the accuracy rate and recall rate.

The recognition results of the five flight states of climb, level flight, circling, turn and descent of the UAV are shown in Table 3.

TABLE III

TABLE OF CLASSIFICATION RESULTS FOR FIVE STATES

Flight states	climbing	level flight	circling	turning	descenting
Training set accuracy rate	97.54%	97.41%	96.13%	95.46%	98.02%
Training set recall	99.25%	98.63%	93.25%	94.63%	98.88%
Training set F1 metric	98.05%	97.77%	95.25%	95.21%	98.27%
Test Set Accuracy Rate	92.65%	89.47%	84.04%	82.74%	92.57%
Test set recall	94.50%	93.50%	81.00%	81.50%	93.50%
Test Set F1 Metric	93.20%	90.94%	82.46	82.36	92.58%

As shown in Figure 6 and Table 3 it can be seen that the

DAGSVM classifier classifies well in climb, level flight and descent recognition, and slightly less well in circling motion states. This classification result shows that the support vector machine model based on directed acyclic graph is feasible in solving the multi-flight state recognition problem.

Finally, the five flight states of the UAV were identified using a random forest model. The training set had 100% accuracy and the test set had lower accuracy. The DAGSVM algorithm proposed in this paper is compared with the traditional random forest model in the test set, and the comparison results are shown in Fig. 7.

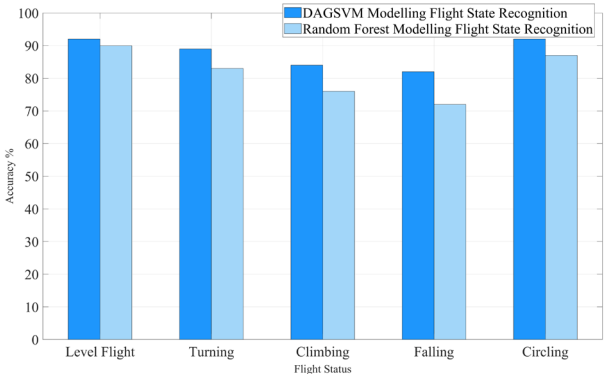

Fig. 7. Algorithm training set accuracy

As shown in Fig. 7, although the accuracy of the previously proposed traditional random forest model on the training set reaches 100% and is higher than that of the DAGSVM model proposed in this paper, the performance of the model on the test set drops significantly. This indicates that the traditional random forest model has a serious overfitting problem when dealing with UAV multi-dimensional data fusion features, whereas the model proposed in this paper is able to effectively extract UAV flight features when dealing with multi-dimensional data, and complete the task of identifying the UAV flight state through these features. This also shows the effectiveness of the DAGSVM algorithm proposed in this paper in handling the UAV multi-sensor data for attitude recognition task.

V. Conclusion

This paper proposes a UAV flight state recognition algorithm based on multi-dimensional data feature fusion. The specific work of this paper is as follows: firstly, data pre-processing, including abnormal data rejection, missing data interpolation and high-frequency noise filtering; secondly, a support vector machine model based on the improved support vector machine model of directed acyclic graph was established to identify the flight states of UAV; finally, the results of the DAGSVM model proposed in this paper are analyzed and validated against the random forest model in the task of identifying the flight state of a UAV with multidimensional features.

The following conclusions can be drawn from the experiment.

1) Designed the UAV record data acquisition system, which can complete the accurate monitoring of UAV data.

2) The trajectory features of UAVs can be effectively extracted using multi-sensor data fusion.

3) The proposed multi-sensor data fusion UAV flight state recognition model in this paper can accurately complete the recognition of UAV flight state.

In future research, we will consider the use of unsupervised machine learning methods for the extraction of UAV trajectory features, as well as research topics related to UAV flight states for multi-aircraft collaboration.

References

[1] E. Kakaletsis et al., “Computer Vision for Autonomous UAV Flight Safety: An Overview and a Vision-based Safe Landing Pipeline Example,” ACM Comput. Surv., vol. 54, no. 9, pp. 1–37, Dec. 2022, doi: 10.1145/3472288.

[2] C. Yan, L. Fu, X. Luo, and M. Chen, “A Brief Overview of Waveforms for UAV Air-to-Ground Communication Systems,” in Proceedings of the 3rd International Conference on Vision, Image and Signal Processing, Vancouver BC Canada: ACM, Aug. 2019, pp. 1–7. doi: 10.1145/3387168.3387203.

[3] D. Orfanus, E. P. de Freitas, and F. Eliassen, “Self-Organization as a Supporting Paradigm for Military UAV Relay Networks,” IEEE Commun. Lett., vol. 20, no. 4, pp. 804–807, Apr. 2016, doi: 10.1109/LCOMM.2016.2524405.

[4] W. W. Greenwood, J. P. Lynch, and D. Zekkos, “Applications of UAVs in Civil Infrastructure,” J. Infrastruct. Syst., vol. 25, no. 2, p. 04019002, Jun. 2019, doi: 10.1061/(ASCE)IS.1943-555X.0000464.

[5] M. Sherman, M. Gammill, A. Raissi, and M. Hassanalian, “Solar UAV for the Inspection and Monitoring of Photovoltaic (PV) Systems in Solar Power Plants,” in AIAA Scitech 2021 Forum, VIRTUAL EVENT: American Institute of Aeronautics and Astronautics, Jan. 2021. doi: 10.2514/6.2021-1683.

[6] A.-I. Siean, R.-D. Vatavu, and J. Vanderdonckt, “Taking That Perfect Aerial Photo: A Synopsis of Interactions for Drone-based Aerial Photography and Video,” in ACM International Conference on Interactive Media Experiences, Virtual Event USA: ACM, Jun. 2021, pp. 275–279. doi: 10.1145/3452918.3465484.

[7] Y. Xia, G. Ye, S. Yan, Z. Feng, and F. Tian, “Application Research of Fast UAV Aerial Photography Object Detection and Recognition Based on Improved YOLOv3,” J. Phys.: Conf. Ser., vol. 1550, no. 3, p. 032075, May 2020, doi: 10.1088/1742-6596/1550/3/032075.

[8] Y. Liu and S. Liu, “Design and Implementation of Farmland Environment Monitoring System Based on Micro Quadrotor UAV,” J. Phys.: Conf. Ser., vol. 2281, no. 1, p. 012005, Jun. 2022, doi: 10.1088/1742-6596/2281/1/012005.

[9] M. Zhang, H. Wang, and J. Wu, “On UAV source seeking with complex dynamic characteristics and multiple constraints: A cooperative standoff monitoring mode,” Aerospace Science and Technology, vol. 121, p. 107315, Feb. 2022, doi: 10.1016/j.ast.2021.107315.

[10] M. Corbetta, P. Banerjee, W. Okolo, G. Gorospe, and D. G. Luchinsky, “Real-time UAV Trajectory Prediction for Safety Monitoring in Low-Altitude Airspace,” in AIAA

Aviation 2019 Forum, Dallas, Texas: American Institute of Aeronautics and Astronautics, Jun. 2019. doi: 10.2514/6.2019-3514.

[11] P. Banerjee and M. Corbetta, "Uncertainty Quantification of Expected Time-of-Arrival in UAV Flight Trajectory," in AIAA AVIATION 2021 FORUM, VIRTUAL EVENT: American Institute of Aeronautics and Astronautics, Aug. 2021. doi: 10.2514/6.2021-2380.

[12] M. Zwick, M. Gerdts, and P. Stütz, "Sensor Model-Based Trajectory Optimization for UAVs Using Nonlinear Model Predictive Control," in AIAA SCITECH 2022 Forum, San Diego, CA & Virtual: American Institute of Aeronautics and Astronautics, Jan. 2022. doi: 10.2514/6.2022-1286.

[13] 'UAV Trajectory Prediction Based on Flight State Recognition | IEEE Journals & Magazine | IEEE Xplore'. Accessed: Nov. 15, 2023. [Online]. Available: https://ieeexplore.ieee.org/document/10214303

[14] H. G. de Marina, F. Espinosa, and C. Santos, "Adaptive UAV Attitude Estimation Employing Unscented Kalman Filter, FOAM and Low-Cost MEMS Sensors," Sensors, vol. 12, no. 7, pp. 9566–9585, Jul. 2012, doi: 10.3390/s120709566.

[15] R. Kannan, "Orientation Estimation Based on LKF Using Differential State Equation," IEEE Sensors J., vol. 15, no. 11, pp. 6156–6163, Nov. 2015, doi: 10.1109/JSEN.2015.2455496.

[16] Y. Wang, K. Li, Y. Han, and X. Yan, "Distributed multi-UAV cooperation for dynamic target tracking optimized by an SAQPSO algorithm," ISA Transactions, vol. 129, pp. 230–242, Oct. 2022, doi: 10.1016/j.isatra.2021.12.014.

[17] G. Heredia, A. Duran, and A. Ollero, "Modeling and Simulation of the HADA Reconfigurable UAV," J Intell Robot Syst, vol. 65, no. 1–4, pp. 115–122, Jan. 2012, doi: 10.1007/s10846-011-9561-9.

[18] D. Thipphavong and C. Schultz, "The Effect of Rate-of-Climb Uncertainty on an Adaptive Trajectory Prediction Algorithm for Climbing Flights," in 12th AIAA Aviation Technology, Integration, and Operations (ATIO) Conference and 14th AIAA/ISSMO Multidisciplinary Analysis and Optimization Conference, Indianapolis, Indiana: American Institute of Aeronautics and Astronautics, Sep. 2012. doi: 10.2514/6.2012-5418.

[19] Z. Shi et al., "Design of Motor Skill Recognition and Hierarchical Evaluation System for Table Tennis Players," in IEEE Sensors Journal, vol. 24, no. 4, pp. 5303-5315, 15 Feb.15, 2024, doi: 10.1109/JSEN.2023.3346880.

[20] S. Rovinska and N. Khan, "Affective State Recognition with Convolutional Autoencoders," in 2022 44th Annual International Conference of the IEEE Engineering in Medicine & Biology Society (EMBC), Glasgow, Scotland, United Kingdom: IEEE, Jul. 2022, pp. 4664–4667. doi: 10.1109/EMBC48229.2022.9871958.

[21] K. Vellenga, H. J. Steinhauer, A. Karlsson, G. Falkman, A. Rhodin, and A. C. Koppisetty, "Driver Intention Recognition: State-of-the-Art Review," IEEE Open J. Intell. Transp. Syst., vol. 3, pp. 602–616, 2022, doi: 10.1109/OJITS.2022.3197296.

Zhuoyong Shi received his bachelor's degree in electronic information engineering from Xi'an Jiaotong University City College. He is currently pursuing a master's degree in electronic science and technology at Northwestern Polytechnical University, China.

Guoqing Shi obtained his master's degree in system engineering from Northwestern Polytechnical University in March 2004, and a doctor's degree in system engineering from Northwestern Polytechnical University in 2011. He was promoted to associate professor of system engineering discipline of Northwest Polytechnical University.

Jiandong Zhang obtained his master's degree in system engineering from Northwestern Polytechnical University in March 2000, and a doctor's degree in system engineering from Northwestern Polytechnical University in 2005. He was promoted to associate professor of system engineering discipline of Northwest Polytechnical University.

Dinghan Wang received his bachelor's degree in Detection Guidance and Control Technology (Electronics) from Northwestern Polytechnical University. He is currently pursuing a master's degree in System Engineering at Northwestern Polytechnical University, China.

Tianyue Xu received his bachelor's degree in Detection Guidance and Control Technology (Electronics) from Northwestern Polytechnical University. He is currently pursuing a master's degree in Electronic Information at Northwestern Polytechnical University, China.

Longing Ji received his bachelor's degree in detection guidance and control technology from Northwestern Polytechnical University. He is currently pursuing a master's degree in control science and engineering at Northwestern Polytechnical University, China.

Yong Wu obtained his bachelor's degree in fire control from Northwestern Polytechnical University in July 1985, and a master's degree in system engineering from Northwestern Polytechnical University in March 1988. He was promoted to professor of system engineering discipline at Northwest Polytechnical University.